CMB anisotropies caused by gravitational waves:
A parameter study

Ruth Durrer[1] and Tina Kahniashvili[2]

April 16, 1999

[1]Université de Genève, Département de Physique Théorique, 4, quai E. Ansermet, CH-1211 Genève 4, Switzerland
[2]Department of Astrophysics, Abastumani Astrophysical Observatory, Kazbegi ave. 2a, 380060 Tbilisi, Georgia

Abstract

Anisotropies in the cosmic microwave background radiation due to gravity waves are investigated. An initial spectrum of gravity waves may have been induced during an epoch of inflation. We study the propagation of such a spectrum in different Friedmann backgrounds with hot and cold dark matter, radiation and, possibly, a cosmological constant. We calculate its imprint as anisotropies on the cosmic microwave background.

We also take into account that massless particles can source gravity waves by their anisotropic stresses. We consider general mixed dark matter models with and without cosmological constant. For a given, scale invariant input spectrum of gravity waves, we determine the dependence of the resulting spectrum of CMB anisotropies on the different parameters of the model.

Keywords: Cosmology: cosmic microwave background; Gravitational waves; Cosmology: large-scale structure of the Universe.

1   Introduction

The theoretical and observational determination of anisotropies in the cosmic microwave background radiation (CMB) has recently attracted a lot of attention. One has justified hopes to measure the CMB anisotropies to a precision of a few percent or better within the next ten years. Furthermore, if initial fluctuations are induced during a primordial inflationary period and no external sources induce perturbations at later times, CMB anisotropies can be calculated by linear cosmological perturbation theory to very good accuracy. Since the detailed results depend not only on the primordial spectrum but also on the parameters of the cosmological model considered, the anisotropy spectrum may provide a mean to determine these parameters to an accuracy of a few percent.

This problem has been extensively investigated mainly for scalar perturbations [1].

As it is well known, also tensor perturbations can by generated during inflation. They play an important role: As shown in [2], the presence of gravitational waves can crucially change the

theoretical predictions of cluster abundance, which is an important test of cosmological models. In particular, power spectra of mixed dark matter (MDM) models normalized to the COBE 4-year data [4] provide cluster abundances higher than observed. This is one of the difficulties of standard MDM models. Taking into account a gravitational wave contribution, this inconsistency can be circumvented. Hence, the question how gravitational wave contributions depend on model parameters is very important.

Here we discuss the model dependence of anisotropies due to gravitational waves for models with a total density parameter $\Omega = 1$ which are thus spatially flat. However, we vary the contributions of cold dark matter (CDM), hot dark matter (HDM) and a cosmological constant, which are given in terms of the parameters Ω_C, Ω_H and Ω_Λ. We also vary the number of degrees of freedom for massless neutrinos and hot particles.

We consider a fixed input spectral index $n = 0$ from inflation. For a general input spectrum $\langle |h(t_{in}, k)|^2 \rangle = A(k)^2 k^{-3}$, our output spectrum $\langle |\dot{h}(t, k)|^2 \rangle$ has to be multiplied by $|A(k)|^2$.

In Section 2 we present the perturbation equations and describe the models considered in this work. In Section 3 we discuss our results and we conclude in Section 4. The non-trivial relation between the temperature anisotropy spectrum, C_ℓ, and the metric fluctuation spectrum $\langle h_{ij}(t, \mathbf{k}) h_{lm}(t', \mathbf{k})^* \rangle$ for tensor perturbations is derived in the appendix.

Notation: The Friedmann metric is given by $a^2(-dt^2 + \gamma_{ij}dx^i dx^j)$, where a denotes the scale factor, t is conformal time, and γ is the metric of a three space with constant curvature K. We shall consider a spatially flat universe, the case $K = 0$ exclusively. An over-dot stands for derivative with respect to conformal time t, while prime denotes the derivative with respect to $kt \equiv x$.

2   The models

The basics of linear perturbations of Friedmann universes are discussed in [5]. We shall adopt the notation of [5] in this work. We want to determine the evolution of tensor perturbations in spatially flat Universes which contain a fraction of cold dark matter (CDM), hot dark matter (HDM) and a cosmological constant Λ, such that: $\Omega_0 = \Omega_H + \Omega_C + \Omega_\Lambda = 1$, where $\Omega_\bullet$ denotes the density parameter today, i.e. at t_0. We neglect the contribution of photons, massless neutrini and baryons (which may be included in CDM) to Ω_0.

The expansion of the Universe is described by the Friedmann equation for the scale factor:

$$\left(\frac{\dot{a}}{a} \right)^2 = \frac{8\pi}{3} G \rho_M a^2 + \frac{1}{3} \Lambda a^2 \tag{1}$$

where ρ_M is the total density of matter in the Universe, $\rho_M = \rho_C + \rho_H + \rho_{\nu_0} + \rho_\gamma$. Here ρ_γ denotes the density of photons, ρ_{ν_0} is the density of massless neutrini and ρ_C, ρ_H denote the densities of CDM and HDM respectively.

The metric element for a Friedmann universe with tensor perturbations is given by:

$$ds^2 = a^2(t)(-dt^2 + (\delta_{ij} + 2h_{ij}^T)dx^i dx^j) \tag{2}$$

where we choose $c = 1$, t is conformal time and $a(t)$ denotes the scale factor. For tensor perturbations, the metric fluctuations h_{ij}^T satisfy the conditions

$$h_i^{Ti} = 0, \qquad h_i^{Tj} k^i = 0 \tag{3}$$

where $\mathbf{k}$ is the wave vector which may be set equal to $(0, 0, k)$, such that the conditions (3) reduce to

$$h_{11}^T = -h_{22}^T, \qquad \text{and} \qquad h_{i3}^T = h_{3i}^T = 0 . \tag{4}$$

We describe dynamics of tensor perturbations in a medium containing collision-less particles, whose anisotropic stresses are not damped by collisions. As long as the collision-less component is relativistic, it provides a source for gravitational waves. The evolution equation for tensor perturbations of the metric is given by [5]:

$$\ddot{h}_{ij}^T + 2\frac{\dot{a}}{a}\dot{h}_{ij}^T + k^2 h_{ij}^T = 8\pi G a^2 p \Pi_{ij} \; . \tag{5}$$

Here p is the pressure of the collision-less component and Π denotes the tensor contribution to the anisotropic stresses, which in our case are due to the presence of relativistic, collision-less particles. Denoting the tensor part of the perturbed distribution function of the collision-less component by F, Π is given by

$$\Pi_{ij} = \frac{1}{pa^4} \int \frac{v^4}{q} (n_i n_j - 1/3\delta_{ij}) F dv d\Omega \tag{6}$$

where n_i is a spatial unit vector, denoting the photon directions, v is the redshift corrected velocity and q the redshift corrected energy of the collision-less particles (see [5]). In the case of massless particles (massless neutrini) $q \equiv v$. Liouville's equation leads to the following perturbation equation for F [5],

$$q\dot{F} + vn^j k_j F = qvn^i n_j \dot{h}_i^{Tj} \frac{df}{dv} \; , \tag{7}$$

f denotes the unperturbed distribution function.

The set of Eqs. (1) to (7) fully describes the evolution of tensor perturbations in media containing perfect fluids and collision-less particles. In our models we have in principle three kinds of collision-less particles: Hot dark matter, massless neutrini and, after recombination, the photons. Studying the initial conditions, we shall find that for the growing mode anisotropic stresses are extremely small on super horizon scales. However, when the scales relevant for tensor CMB anisotropies ($\lambda \gg t_{dec}$) enter the horizon, $t \gg t_{dec}$ HDM particles are already non relativistic. We may thus neglect their contribution to anisotropic stresses. Hence, we just consider the pressure anisotropy from massless neutrini and, after recombination, from the photons themselves.

For massless particles we can simplify Eqs. (6) and (7) by introducing the brightness perturbation M

$$M \equiv \frac{4\pi}{\rho_{\nu_0} a^4} \int_0^\infty F v^3 dv \tag{8}$$

In terms of M Liouville's equation (7) becomes:

$$\dot{M} + in^j k_j M = -4n^l n^j \dot{h}_{lj}^T \tag{9}$$

and the anisotropic stresses are given by:

$$\Pi_{ij} = \frac{3}{4\pi} \int (n_i n_j - 1/3\delta_{ij}) M d\Omega \; . \tag{10}$$

Equations (5),(9),(10) for perturbations and eqn. (1) for scale factor together with the usual equations determining ρ_C, ρ_H ρ_{ν_0} and ρ_γ form the closed system of ordinary differential equation which we have solved.

We assume standard inflation according to which the initial amplitude of gravitational waves is independent of scale i.e., $\langle |h(t_{in}, k)|^2 \rangle \propto k^{-3}$.

Each solution of Eqs. (5),(9) and (10) can be presented as a sum of growing and decaying modes and an infinite number of modes corresponding to perturbations of the collision-less medium [6]. We are only interested in the growing mode which is given by the initial condition $h_{ij}^T(t \to 0) =$const. and $\dot{h}_{ij}(t \to 0) = 0$.

If $\dot{h}_{ij} = 0$, Eq. (9) does not admit a tensor contribution to M. In this case, $M \propto \exp(i\mathbf{n} \cdot \mathbf{k})$ and all components of the induced anisotropic stress normal to $\mathbf{k}$ vanish. Therefore, the correct (tensorial) initial condition for M is $M(t \to 0) = 0$ and also $\Pi_{ij}(t \to 0) = 0$.

These initial values remain unchanged as long as $kt \ll 1$. Assuming, e.g. spherical polarization and a flat spectrum from inflation, at some early time, $kt \ll 1$ for all wavelengths considered, we thus choose the initial conditions

$$\langle |h_{11}^T|^2 \rangle = \langle |h_{12}^T|^2 \rangle = \langle |h|^2 \rangle = A^2 k^{-3}, \quad \Pi_{11} = \Pi_{12} = 0, \quad M = 0 , \tag{11}$$

where A is the amplitude of gravitational waves. It is easy see that on superhorizon scales ($kt \ll 1$), $h =$const. and the evolution of gravitational waves and as a result $\Delta T/T$ are independent of the model parameters. For scales $kt \approx 1$, the metric perturbations begin to oscillate and eventually ($kt \gg 1$) damp away (see Figs. 1 and 2). The non-zero $\dot h$ then induces anisotropic stresses via Eqs.(9) and (10). Very often, these anisotropic stresses have been neglected in the literature. Here we find that their effect is indeed very small. There is typically about 1% additional damping due to the loss of some gravitational wave energy into anisotropic stresses.

The main model dependence is the modification of the damping term ($\dot a/a$) in the different backgrounds considered.

We want to determine the CMB anisotropy spectrum induced by gravitational waves. Using that the brightness perturbation M for photons is actually

$$M = 4\frac{\Delta T}{T} .$$

we obtain by integrating Eq. (9) for photons[1]

$$\frac{\Delta T}{T}(t_0, \mathbf{k}, \mathbf{n}) = \exp(i\mathbf{k} \cdot \mathbf{n} t_0) \int_{t_{dec}}^{t_0} n^i n^j \dot h_{ij}^T(t, \mathbf{k}) \exp(-i\mathbf{k} \cdot \mathbf{n} t) dt . \tag{12}$$

The power spectrum, C_l of the CMB anisotropies can defined by the expansion of the correlation function into spherical harmonics.

$$C(\cos\theta) = \left\langle \frac{\Delta T}{T}(t_0, x_0, \mathbf{n}) \cdot \frac{\Delta T}{T}(t_0, x_0, \mathbf{n}') \right\rangle_{(\mathbf{n} \cdot \mathbf{n}') = \cos\theta} = \frac{1}{4\pi}\Sigma(2l + 1)C_\ell P_\ell(\cos\theta) \tag{13}$$

A somewhat lengthy calculation relates the gravitational wave spectrum $|\dot h(t, k)|^2$ via Eqs. (12) and (13) to the C_ℓ's. Taking into account the conditions (3), it is possible to split this integral into two part coming from h_{11}^T and h_{12}^T. If we assume initially $\langle |h_{11}^T|^2 \rangle = \langle |h_{12}^T| \rangle = |H|^2$ (no polarization), the two terms are equal.

$$C_\ell = \frac{2}{\pi} \int dk k^2 |I(\ell, k)|^2 \ell(\ell - 1)(\ell + 1)(\ell + 2) , \tag{14}$$

with

$$I(\ell, k) = \int_{t_{dec}}^{t_0} dt \dot H(t, k) \frac{j_\ell((k(t_0 - t))}{(k(t_0 - t))^2} \tag{15}$$

(see also [7]), where j_ℓ denotes the spherical Bessel function of order ℓ. A self contained derivation of Eq. (15) is presented in the appendix.

Before we come to a description of the model dependence of the results, let us discuss the expected behavior in general. For a rough discussion we may neglect the anisotropic stresses in Eq. (5). We first consider large scales which enter the horizon only after decoupling, $kt_{dec} \ll 1$. These scales contribute to $|I(\ell, k)|^2$ by roughly $A^2 k^{-3} j_\ell^2(kt_0)/\ell^4$. Inserting such a contribution in Eq. (14) and integrating over k yields

$$\ell^2 C_\ell \sim A^2 . \tag{16}$$

---

[1] Prior to and during recombination, photons Thomson scatter with the electrons. For photons, we thus, in principle, have a collision term on the right hand side of Eq. (9). But this is only important on relatively small angular scales, $\ell \gtrsim 500$, which we are not investigating here. We thus neglect the collision term.

The integration over k is only justified if the main contribution to j_ℓ^2 comes from the regime, where $kt_{dec} \ll 1$, in other words, if $kt_0 \sim \ell$ for a value of k with $kt_{dec} \ll 1$, which is equivalent to $\ell \ll t_{dec}/t_0 \sim 50$.

Perturbations on small scales, $kt_{dec} \gg 1$ are damped by a factor of about $(t_{enter}/t_{dec})^2 \sim 1/(kt_{dec})^2$ until decoupling[2]. Here $t_{enter} \sim 1/k$ denotes the scale at which the mode k enters the horizon. Since the main contribution to C_ℓ comes from the scales k with $kt_0 \sim \ell$, we obtain an approximate behavior of

$$\ell^2 C_\ell \sim A^2 \left(\frac{50}{\ell}\right)^4 \quad \text{for } \ell \gg t_{dec}/t_0 \sim 50 \ . \tag{17}$$

This analysis explains the generic behavior of the curves shown in Fig. 3.

Let us now come to a more detailed analysis. Having calculated the metric perturbations h_{ij}^T numerically, we can determine the CMB fluctuation spectrum according to Eq. (15) by means of numerical integration (we have used 60 to 100 point Gauss-Lagrange and Gauss-Laguerre integrations) and investigate it's dependence on the model parameters.

3   Results

We have solved Eqs. (5), (9) and (10) numerically for $t_{in} \leq t \leq t_0$ choosing the initial conditions of the growing mode and unpolarized, isotropic waves, $\langle |h_{11}^T|^2 \rangle = \langle |h_{12}^T|^2 \rangle$. For a given model of inflationary initial perturbations, our results would have to be properly weighted and added to the scalar C_ℓ's.

We have chosen a flat initial spectrum, such that $h_{in}^T = Ak^{-3/2}$ and $\dot{h}_{in} = 0$.

We have investigated 80 models varying the five parameters $(h_0, \Omega_\Lambda, \Omega_H/\Omega_C, \beta_\nu, \beta_H)$, where h_0 is the Hubble parameter H_0 in units of 100km/s/Mpc, β_ν denotes the number of degrees of freedom in massless neutrini and β_H is the corresponding number for hot dark matter particles.

All the models lead to similar gravity wave induced anisotropies which, for reasonable parameter choices, differ by less than about 10%. The changes due to anisotropic stresses are extremely small, on the order of 1% or less. The main difference is caused by a non-zero cosmological constant, which enhances the damping at late times and thus leads to somewhat smaller perturbation amplitudes (see also [8]). A similar effect is obtained if we increase the Hubble parameter. Hot dark matter does not induce significant changes since, at times when the wavelengths leading to substantial CMB anisotropies enter the horizon, hot dark matter is already non-relativistic, resulting in nearly the same expansion law as cold dark matter. In Fig. 1, we show the dependence of $\dot{h}(t, k)$ for fixed k as a function of time varying several model parameters. We have chosen $k = 20/t_0$, which contributes mainly to an angle of $\theta \sim 6^o$ in the sky, or to the C_ℓ's with $\ell \sim 10$ to 20. For some of these models we also show $\dot{h}(t, k)$ as a function of k for fixed time $t = t_0/2$ in Fig. 2.

The solid line always shows standard CDM, i.e. $\Omega_C = 1$ and $\beta_\nu = 6$ for comparison. The maximum amplitudes for standard CDM and CDM+Λ differ by more than 30%, while the mixed dark matter models show differences of about 1% only. The somewhat weaker damping due to the absence of the anisotropic stresses provided by a massless neutrino component and the decrease of $\dot{a}/a$ leads to the slight increase in amplitude for mixed dark matter models with $\Omega_H = 0.5$. This result does not change if we increase the amount of hot dark matter. However, if we decrease Ω_H to 0.3 or less no amplitude change is left and only a small decrease in wavelengths builds up after about one oscillation. Due to the smallness of these effects, which remain of the order of 1% to 2% when translated into the C_ℓ's, we disregard mixed dark matter models in what follows and claim that, on the level of 1% accuracy, MDM and CDM lead to the same gravitational wave spectra.

---

[2]Here we neglect the short matter dominated period before decoupling and approximate the damping factor by its behavior in the radiation dominated era, $(\dot{a}/a) \sim 1/t$.

Changing the number of degrees of freedom in massless neutrini or HDM also induces very small differences of the order of 1%.

Taking into account that an experiment always just measures the sum of tensor and scalar contributions and first has to disentangle the probably significantly smaller gravitational wave contribution, we can disregard such small effects, even if the experimental error is as small as possible, *i.e.* dominated by cosmic variance.

The relevant parameters to be considered are thus $\Omega_M = \Omega_C + \Omega_H$, Ω_Λ and h_0.

In the k dependence of $\dot{h}$ an additional effect comes into play: Due to the model dependence of t_0, the oscillations in $\dot{h}$ at a fixed fraction $t = ft_0$ of t_0 have different wavelengths if measured in units of t_0. Models with a larger cosmological constant oscillate slower in kt_0 than models with small cosmological constant. Therefore, the cancelation due to oscillations in the integral (15) is more severe for models with small cosmological constant. This effect finally dominates over the larger amplitude of $\dot{h}$ which models with large Λ actually have. In Fig. 3 we show the C_ℓ spectra for several models and in a Fig. 4 the relative differences are indicated. The Λ-models shown in frames (a) of Figs. 3 and 4 show a slightly increasing amplitude with increasing Λ. As can be seen in frames (b) of Figs. 3 and 4, increasing h_0, which does not lead to an increase in the relative oscillation frequency, just decreases the fluctuations due to stronger damping. The detailed model parameters of the frames (b) are just given for information. The only parameters which really matter are Ω_Λ and h_0. The variations induced by changing the other parameters are on the 1% level and thus swamped by cosmic variance.

The variation of the tensor C_ℓ spectrum for different cosmological models with fixed Hubble parameter which are not already excluded by other observations than CMB anisotropies never exceed 10% for $\ell < 60$, while variations of the Hubble parameter can lead to changes in the spectrum of up to 15%.

4   Conclusions

We have calculated the tensor contribution to the CMB anisotropies in mixed dark matter models with and without cosmological constant. We have included a previously neglected source term in the evolution equation for metric perturbations. Our findings are however quite modest: By reasons of cosmic variance, the statistical relative error in C_ℓ measured from only one point in the universe is always $1/\sqrt{2\ell + 1}$. This is a very significant uncertainty, especially for the gravitational wave contribution which peaks around $\ell \sim 20$ and has already dropped by a factor of about 2 at $\ell = 60$ (see Fig. 3).

In non of the considered models the influence of the anisotropic stress source becomes large enough to induce a difference in the C_ℓ spectrum which is larger than cosmic variance. The same is true for hot dark matter contributions. Only an extremely large cosmological constant or a difference in the Hubble parameter can induce changes in the gravitational wave spectrum which are in principle observable but nevertheless small.

This finding has one negative and one positive aspect: Unfortunately, the gravitational wave contribution does not contain detailed information about the cosmological parameters considered here and can thus not be used to measure them with high accuracy. On the other hand, since this contribution is so model independent, it conserves its information about the initial condition and thus about the amplitude and spectral index which it inherited during, e.g., an inflationary epoch.

Appendix: The C_ℓ's from gravitational waves

We consider metric perturbations which are produced by some isotropic random process (for example during inflation). After production, they evolve according to a deterministic equation of motion. The correlation functions of $h_{ij}(\mathbf{k}, t)$ have to be of the form

$$
\begin{aligned}
\langle h_{ij}(\mathbf{k}, t) h_{lm}^*(\mathbf{k}, t') \rangle \quad = \quad & [k_i k_j k_l k_m H_1(k, t, t') + \\
& (k_i k_l \delta_{jm} + k_i k_m \delta_{jl} + k_j k_l \delta_{im} + k_j k_m \delta_{il}) H_2(k, t, t') + \\
& k_i k_j \delta_{lm} H_3(k, t, t') + k_l k_m \delta_{ij} H_3^*(k, t', t) + \\
& + \delta_{ij} \delta_{lm} H_4(k, t, t') + (\delta_{il} \delta_{jm} + \delta_{im} \delta_{jl}) H_5(k, t, t')] .
\end{aligned}
\tag{A1}
$$

Here the functions H_a are functions of the modulus $k = |\mathbf{k}|$ only. Furthermore, all of them except H_3 are hermitian in t and t'. This is the most general ansatz for an isotropic correlation tensor satisfying the symmetries required. To project out the tensorial part of this correlation tensor we act on h_{ij} it with the tensor projection operator,

$$
\begin{aligned}
T_{ij}{}^{ab} \quad &= \quad (P_{il} P_{jm} - (1/2) P_{ij} P_{lm}) P^{ma} P^{lb} \quad \text{with} \tag{A2} \\
P_{ij} \quad &= \quad \delta_{ij} - \hat{k}_i \hat{k}_j . \tag{A3}
\end{aligned}
$$

This yields

$$
\begin{aligned}
\langle h_{ij}^{(T)}(\mathbf{k}, t) h_{lm}^{(T)*}(\mathbf{k}, t') \rangle = \\
H_5(k, t, t')[\delta_{il} \delta_{jm} + \delta_{im} \delta_{jl} - \delta_{ij} \delta_{lm} + k^{-2}(\delta_{ij} k_l k_m + \\
\delta_{lm} k_i k_j - \delta_{il} k_j k_m - \delta_{im} k_l k_j - \delta_{jl} k_i k_m - \delta_{jm} k_l k_i) + \\
k^{-4} k_i k_j k_l k_m] .
\end{aligned}
\tag{A4}
$$

From Eq. (12), we then obtain

$$
\begin{aligned}
\left\langle \frac{\Delta T}{T}(\mathbf{n}) \frac{\Delta T}{T}(\mathbf{n}') \right\rangle \equiv \frac{1}{V} \int d^3 x \left(\frac{\Delta T}{T}(\mathbf{n}, \mathbf{x}) \frac{\Delta T}{T}(\mathbf{n}', \mathbf{x}) \right) = \\
\left(\frac{1}{2\pi} \right)^3 \int k^2 dk d\Omega_{\hat{\mathbf{k}}} \int_{t_{dec}}^{t_0} dt \int_{t_{dec}}^{t_0} dt' \exp(i\mathbf{k} \cdot \mathbf{n}(t_0 - t)) \exp(-i\mathbf{k} \cdot \mathbf{n}(t_0 - t')) \cdot \\
\left[\langle \dot{h}_{ij}^{(T)}(t, \mathbf{k}) \dot{h}_{lm}^{(T)*}(t', \mathbf{k}) \rangle n_i n_j n_l' n_m' \right] .
\end{aligned}
\tag{A5}
$$

Here $d\Omega_{\hat{\mathbf{k}}}$ denotes the integral over directions in $\mathbf{k}$ space. We use the normalization of the Fourier transform

$$
\hat{f}(\mathbf{k}) = \frac{1}{\sqrt{V}} \int d^3 x \exp(i\mathbf{x} \cdot \mathbf{k}) f(\mathbf{x}) , \quad f(\mathbf{x}) = \frac{1}{(2\pi)^3} \int d^3 k \exp(-i\mathbf{x} \cdot \mathbf{k}) \hat{f}(\mathbf{k}) ,
$$

where V is an (arbitrary) normalization volume.

We now introduce the form (A4) of $< h^{(T)} h^{(T)} >$. We further make use of the assumption that the perturbations have been created at some early epoch, e.g. during an inflationary phase, after which they evolved deterministically. The function $H_5(k, t, t')$ is thus a product of the form

$$
H_5(k, t, t') = H(k, t) \cdot H^*(k, t') .
\tag{A6}
$$

Introducing this in Eq. (A5) yields

$$
\begin{aligned}
\left\langle \frac{\Delta T}{T}(\mathbf{n}) \frac{\Delta T}{T}(\mathbf{n}') \right\rangle = \\
\left(\frac{1}{2\pi} \right)^3 \int k^2 dk d\Omega_{\hat{\mathbf{k}}} \left[(\mathbf{n} \cdot \mathbf{n}')^2 - 1 + \mu'^2 + \mu^2 - 4\mu\mu'(\mathbf{n} \cdot \mathbf{n}') + \mu^2 \mu'^2 \right] \cdot \\
\int_{t_{dec}}^{t_0} dt \int_{t_{dec}}^{t_0} dt' \left[\dot{H}(k, t) \dot{H}^*(k, t') \exp(ik\mu(t_0 - t)) \exp(-ik\mu'(t_0 - t')) \right] ,
\end{aligned}
\tag{A7}
$$

7

where $\mu = (n \cdot \hat{\mathbf{k}})$ and $\mu' = (n' \cdot \hat{\mathbf{k}})$. To proceed, we use the identity [9]

$$\exp((ik\mu(t_0 - t)) = \sum_{r=0}^{\infty}(2r + 1)i^r j_r(k(t_0 - t))P_r(\mu) . \tag{A8}$$

Here j_r denotes the spherical Bessel function of order r and P_r is the Legendre polynomial of degree r.

Furthermore, we replace each factor of μ in Eq. (A7) by a derivative of the exponential $\exp(ik\mu(t_0 - t))$ with respect to $k(t_0 - t)$ and correspondingly with μ'. We then obtain

$$\left\langle \frac{\Delta T}{T}(\mathbf{n})\frac{\Delta T}{T}(\mathbf{n}') \right\rangle =$$

$$\left(\frac{1}{2\pi}\right)^3 \sum_{r,r'}(2r + 1)(2r' + 1)i^{(r-r')}\int k^2 dk d\Omega_{\hat{\mathbf{k}}}P_r(\mu)P_{r'}(\mu') \times$$

$$\left[2(\mathbf{n} \cdot \mathbf{n}')^2 \int dt dt' j_r(k(t_0 - t))j_{r'}(k(t_0 - t'))\dot{H}(k,t)\dot{H}^*(k,t') \right.$$

$$- \int dt dt' [j_r(k(t_0 - t))j_{r'}(k(t_0 - t')) + j_r''(k(t_0 - t))j_{r'}(k(t_0 - t')) +$$

$$j_r(k(t_0 - t))j_{r'}''(k(t_0 - t')) - j_r''(k(t_0 - t))j_{r'}''(k(t_0 - t'))]\dot{H}(k,t)\dot{H}^*(k,t')$$

$$\left. -4(\mathbf{n} \cdot \mathbf{n}')\int dt dt' j_r'(k(t_0 - t))j_{r'}'(k(t_0 - t'))\dot{H}(k,t)\dot{H}^*(k,t') \right] . \tag{A9}$$

Here only the Legendre polynomials, $P_r(\mu)$ and $P_{r'}(\mu')$ depend on the direction $\hat{\mathbf{k}}$. To perform the integration $d\Omega_{\hat{\mathbf{k}}}$, we use the addition theorem for the spherical harmonics Y_{rs},

$$P_r(\mu) = \frac{4\pi}{(2r + 1)}\sum_{s=-r}^{r} Y_{rs}(\mathbf{n})Y_{rs}^*(\hat{\mathbf{k}}) . \tag{A10}$$

The orthogonality of the spherical harmonics then yields

$$(2r + 1)(2r' + 1)\int d\Omega_{\hat{\mathbf{k}}}P_r(\mu)P_{r'}(\mu') =$$

$$16\pi^2\delta_{rr'}\sum_{s=-r}^{r} Y_{rs}(\mathbf{n})Y_{rs}^*(\mathbf{n}') =$$

$$4\pi\delta_{rr'}P_r(\mathbf{n} \cdot \mathbf{n}') . \tag{A11}$$

In Eq. (A9) the integration over $d\Omega_{\hat{\mathbf{k}}}$ then leads to terms of the form $(\mathbf{n} \cdot \mathbf{n}')P_r(\mathbf{n} \cdot \mathbf{n}')$ and $(\mathbf{n} \cdot \mathbf{n}')^2 P_r(\mathbf{n} \cdot \mathbf{n}')$. To reduce them, we use

$$xP_r(x) = \frac{r + 1}{2r + 1}P_{r+1} + \frac{r}{2r + 1}P_{r-1} . \tag{A12}$$

Applying this and its iteration for $x^2 P_r(x)$, we obtain

$$\langle \frac{\Delta T}{T}(\mathbf{n})\frac{\Delta T}{T}^*(\mathbf{n}') \rangle =$$

$$\frac{1}{2\pi^2}\sum_r(2r + 1)\int k^2 dk \int dt dt' \dot{H}(k,t)\dot{H}^*(k,t')\Big\{$$

$$\left[\frac{2(r + 1)(r + 2)}{(2r + 1)(2r + 3)}P_{r+2} + \frac{1}{(2r - 1)(2r + 3)}P_r + \frac{2r(r - 1)}{(2r - 1)(2r + 1)}P_{r-2} \right] \times$$

$$j_r(k(t_0 - t))j_r(k(t_0 - t')) - P_r[j_r(k(t_0 - t))j_r''(k(t_0 - t'))$$
$$+j_r(k(t_0 - t'))j_r''(k(t_0 - t)) - j_r''(k(t_0 - t))j_{r'}''(k(t_0 - t'))]$$
$$-4\left[\frac{r+1}{2r+1}P_{r+1} + \frac{r}{2r+1}P_{r-1}\right]j_r'(k(t_0 - t))j_r'(k(t_0 - t'))\bigg\} \,, \tag{A13}$$

where the argument of the Legendre polynomials, $\mathbf{n} \cdot \mathbf{n}'$, has been suppressed. Using the relations

$$j_r' = -\frac{r+1}{2r+1}j_{r+1} + \frac{r}{2r+1}j_{r-1} \tag{A14}$$

for Bessel functions, and its iteration for j'', we can rewrite Eq. (A13) in terms of the Bessel functions j_{r-2} to j_{r+2}.

To proceed we use the definition of C_ℓ:

$$\left\langle \frac{\Delta T}{T}(\mathbf{n}) \cdot \frac{\Delta T}{T}(\mathbf{n}') \right\rangle_{(\mathbf{n}\cdot\mathbf{n}')=\cos\theta} = \frac{1}{4\pi}\Sigma(2l+1)C_\ell P_\ell(\cos\theta) \tag{A15}$$

If we expand

$$\frac{\Delta T}{T}(\mathbf{n}) = \sum_{\ell,m} a_{\ell,m} Y_{\ell,m}(\mathbf{n}) \tag{A16}$$

and use the orthogonality of the spherical harmonics as well as the addition theorem, Eq. (A10), we get

$$C_\ell = \langle a_{\ell,m} a_{\ell,m}^* \rangle \,. \tag{A17}$$

We thus have to determine the correlators

$$\langle a_{\ell m} a_{\ell'm'}^* \rangle = \int d\Omega_{\mathbf{n}} \int d\Omega_{\mathbf{n}'} \left\langle \frac{\Delta T}{T}^* \frac{\Delta T}{T} \right\rangle Y_{\ell m}^*(\mathbf{n}) Y_{\ell'm'}(\mathbf{n}') \,. \tag{A18}$$

Inserting our result (A13), we obtain the somewhat lengthy expression

$$\langle a_{\ell m} a_{\ell'm'}^* \rangle =$$
$$\frac{2}{\pi}\delta_{\ell\ell'}\delta_{mm'} \int dk k^2 \int dt dt' \dot{H}(k,t)\dot{H}^*(k,t')\Big\{$$
$$j_l(k(t_0 - t))j_l(k(t_0 - t')) \times$$
$$\bigg(\frac{1}{(2\ell-1)(2\ell+3)} + \frac{2(2\ell^2+2\ell-1)}{(2\ell-1)(2\ell+3)} + \frac{(2\ell^2+2\ell-1)^2}{(2\ell-1)^2(2\ell+3)^2}$$
$$-\frac{4\ell^3}{(2\ell-1)^2(2\ell+1)} - \frac{4(\ell+1)^3}{(2\ell+1)(2\ell+3)^2}\bigg)$$
$$-[j_\ell(k(t_0 - t))j_{\ell+2}(k(t_0 - t')) + j_{\ell+2}(k(t_0 - t))j_\ell(k(t_0 - t'))] \times$$
$$\frac{1}{2l+1}\left(\frac{2(\ell+2)(\ell+1)(2\ell^2+2\ell-1)}{(2\ell-1)(2\ell+3)^2} + \frac{2(\ell+1)(\ell+2)}{(2\ell+3)} - \frac{8(\ell+1)^2(\ell+2)}{(2\ell+3)^2}\right)$$
$$-[j_\ell(k(t_0 - t))j_{\ell-2}(k(t_0 - t')) + j_{\ell-2}(k(t_0 - t))j_\ell(k(t_0 - t'))] \times$$
$$\frac{1}{2l+1}\left(\frac{2\ell(\ell-1)(2\ell^2+2\ell-1)}{(2\ell-1)^2(2\ell+3)} + \frac{2\ell(\ell-1)}{(2\ell-1)(2} - \frac{8\ell^2(\ell-1)}{(2\ell-1)^2}\right)$$
$$+j_{\ell+2}(k(t_0 - t))j_{\ell+2}(k(t_0 - t')) \times$$
$$\left(\frac{2(\ell+2)(\ell+1)}{(2\ell+1)(2\ell+3)} - \frac{4(\ell+1)(\ell+2)^2}{(2\ell+1)(2\ell+3)^2} + \frac{(\ell+1)^2(\ell+2)^2}{(2\ell+1)^2(2\ell+3)^2}\right)$$
$$+j_{\ell-2}(k(t_0 - t))j_{\ell-2}(k(t_0 - t')) \times$$
$$\left(\frac{2\ell(\ell-1)}{(2\ell-1)(2\ell+1)} - \frac{4\ell(\ell-1)^2}{(2\ell-1)^2(2\ell+1)} + \frac{\ell^2(\ell-1)^2}{(2\ell-1)^2(2\ell+1)^2}\right)\Big\} \tag{A19}$$

An analysis of the coefficient of each term reveals that this result is equivalent to Eq. (14) with.

$$I(\ell, k) = \frac{j_{\ell+2}(k(t_0 - t))}{(2\ell + 3)(2\ell + 1)} + \frac{2j_\ell(k(t_0 - t))}{(2\ell + 3)(2\ell - 1)} + \frac{j_{\ell-2}(k(t_0 - t))}{(2\ell + 1)(2\ell - 1)} y \tag{A20}$$

$$= \frac{j_\ell(k(t_0 - t))}{(k(t_0 - t))^2} . \tag{A21}$$

References

[1] S. Dodelson, E. Gates and A. Stebbins, *Astrophys.J.* **467**, 10 (1996);
W. Hu, D. Scott, N. Sugijama and M. White, *Phys. Rev.* **D52**, 5498 (1995);
W. Hu, N. Sugijama and J. Silk, Nature, in press (1997).

[2] C.-P. Ma, *Astrophys.J* **471**, 13 (1996)

[3] G.F. Smoot, C.L. Bennett, A. Kogut et al., *Astrophys.J* **396**, L1 (1992)

[4] E.F. Bunn, E. and M. White, *Astrophys.J.* **480**, 6 (1997)

[5] R. Durrer, *Fundamentals in Cosmic Physics* **15**, 209 (1994).

[6] V. I. Khlebnikov *ZhETF* **86**, 13 (1984).

[7] F.F. Abott and M.B. Wise, *Nucl. Phys.* **B244**, 541 (1984).

[8] L. A. Kofman and A. A. Starobinskii *Sov. Astron. Lett.* **11**, 271 (1985);
O. Lahav, P. B. Lilje, J. R. Primack and M. J. Rees *MNRAS* **251**, 128 (1991).

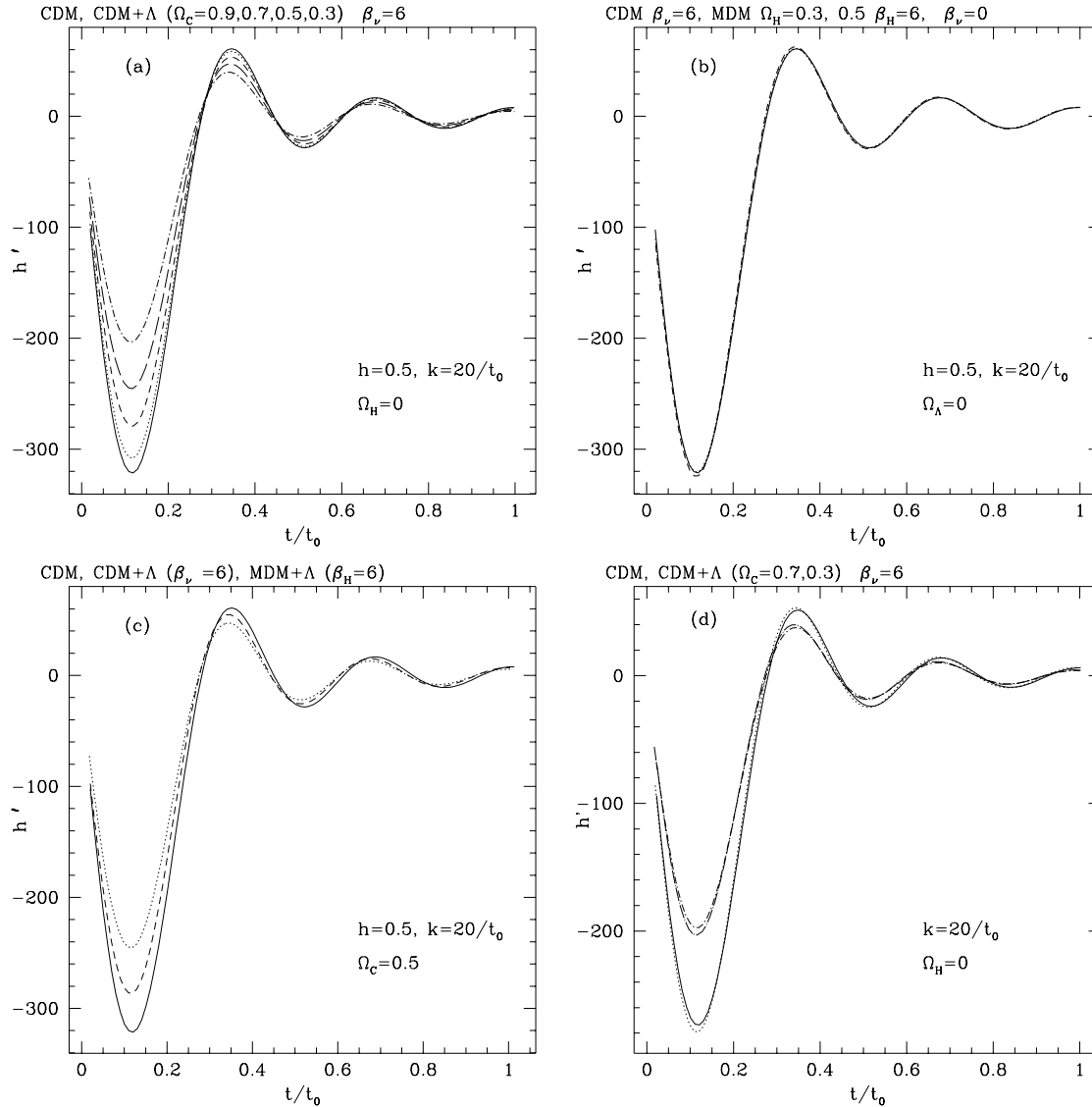[9] M. Abramowitz and I. Stegun, *Handbook of Mathematical Functions*, Dover Publications, New York (1972).

Figure 1: The variable $\dot{h}$ is shown at fixed wave number $k = 20/t_0$ as function of time for different models. In frame (a), we consider models without HDM. The solid line shows pure CDM (with 3 sorts of massless neutrini). The dotted, dashed, long dashed and dash–dotted lines show models with increasing Ω_Λ. In frame (b), mixed dark matter models with $\Omega_H = 0.3$ (dotted) and $\Omega_H = 0.5$ (dashed) are compared with standard CDM (solid line). In frame (c) standard CDM (solid line), with $\Omega_{CDM} = \Omega_\Lambda = 0.5$ (dotted line) and $\Omega_{CDM} = 0.5$, $\Omega_\Lambda = \Omega_H = 0.25$ (dashed line) are shown. In frame (d) we compare $\Omega_\Lambda = 0.3$ models with Hubble parameters $h_0 = 0.5$ (dotted) and $h_0 = 0.75$ (solid); and $\Omega_\Lambda = 0.7$ models with $h_0 = 0.5$ (dash-dotted) and $h_0 = 0.75$ (long-dash-dotted).
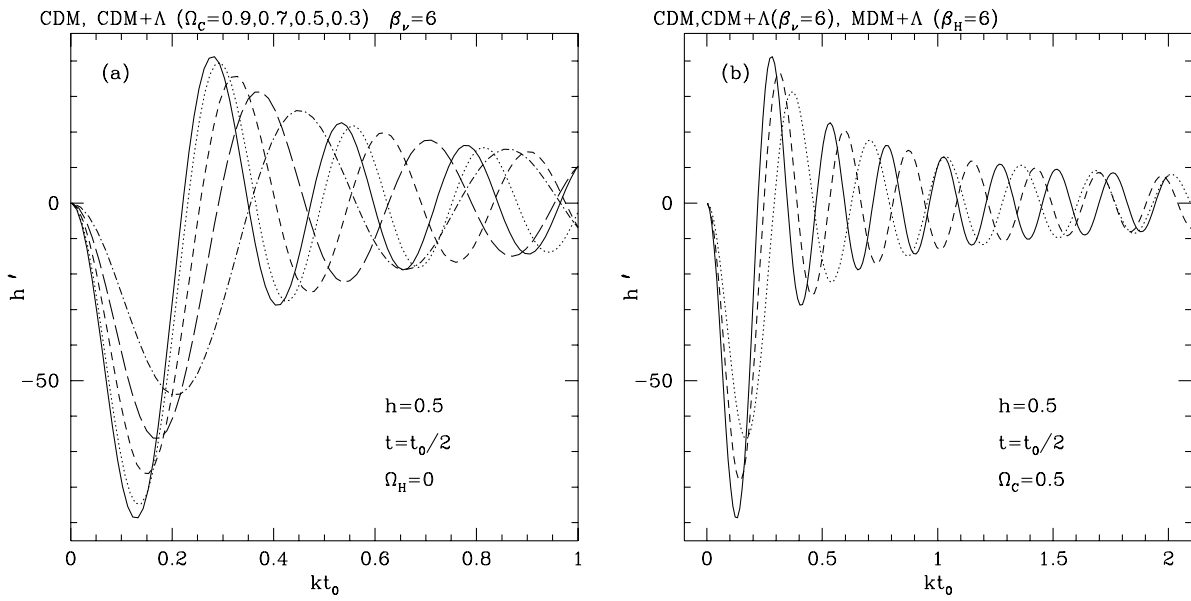
Figure 2: The variable $\dot{h}$ is shown at fixed time, $t = t_0/2$ as function of the wave number k for different models. In frame (a), we consider models without HDM. The solid line shows pure CDM (with 3 sorts of massless neutrini). The dotted, dashed, long dashed and dash–dotted lines show models with increasing Ω_Λ. In frame (b) standard CDM (solid line), with $\Omega_{CDM} = \Omega_\Lambda = 0.5$ (dotted line) and $\Omega_{CDM} = 0.5$, $\Omega_\Lambda = \Omega_H = 0.25$ (dashed line) are shown.
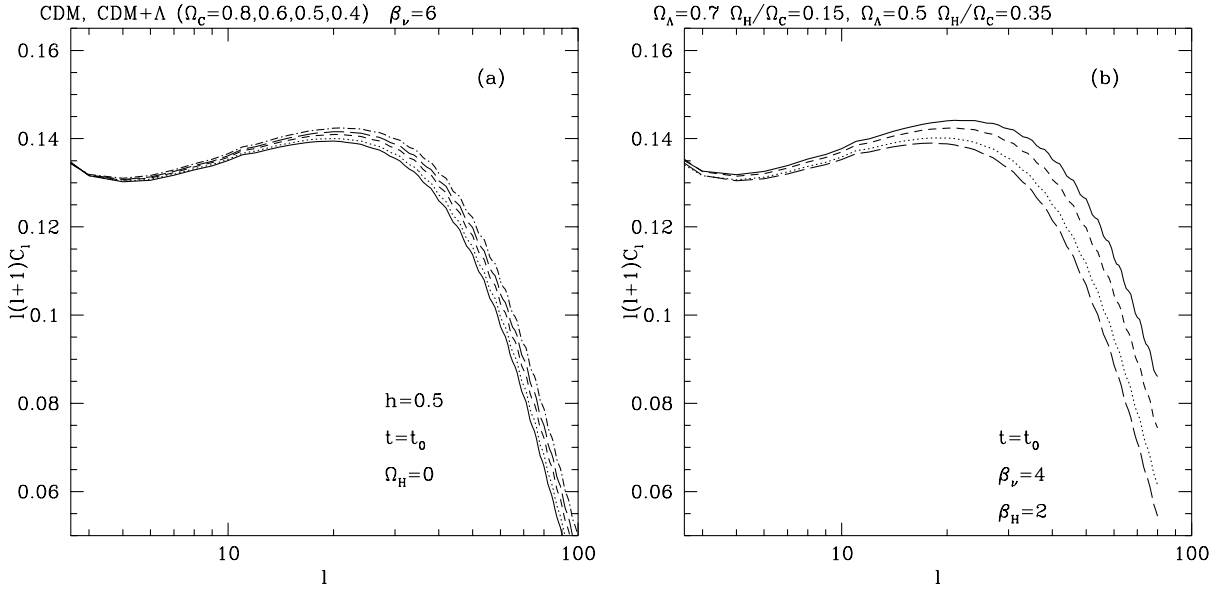
Figure 3: In frame (a), the angular power spectra of CMB anisotropies induced by gravitational waves are shown for models with different values for the cosmological constant. The solid line represents the model $\Omega_\Lambda = 0$ (solid line) and the amplitude increases with increasing Λ. In frame (b), we show the effect of increasing the Hubble parameter. The models chosen are mixed dark matter models with cosmological constant, $\Omega_H/\Omega_{CMD} = 0.15$, $\Omega_\Lambda = 0.7$ with $h_0 = 0.5$ (solid line) and $h_0 = 0.75$ (dotted line); and $\Omega_H/\Omega_{CDM} = 0.35$, $\Omega_\Lambda = 0.5$ with $h_0 = 0.5$ (dashed line) and $h_0 = 0.75$ (long dashes) are shown.
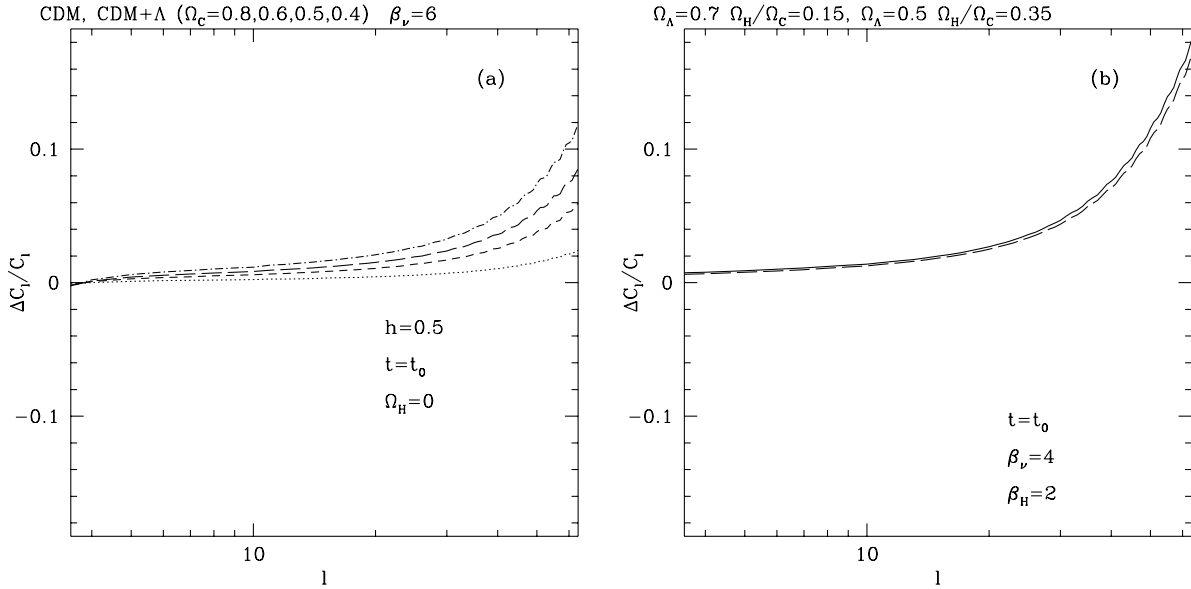

Figure 4: The relative differences for the models given in Fig. 3 are shown. In frame (a) the same line types as in Fig 3a are chosen, and the difference from standard CMB is indicated. In frame (b) The difference between $h_0 = 0.5$ and $h_0 = 0.75$ is shown for the model $\Omega_H/\Omega_{CDM} = 0.35$, $\Omega_\Lambda = 0.5$ (solid line) and $\Omega_H/\Omega_{CMD} = 0.15$, $\Omega_\Lambda = 0.7$ (dashed line).

13